Spatial distribution of deuterium in atmospheric water vapor: diagnosing sources and the mixing of atmospheric moisture

Tsutomu Yamanaka [a,*], Ryosuke Shimizu [b]

[a] *Terrestrial Environment Research Center, University of Tsukuba, Tsukuba 305-8577, Japan*

[b] *Graduate School of Life and Environmental Sciences, University of Tsukuba, Tsukuba 305-8577, Japan*

Submitted to: *Geochimica et Cosmochimica Acta*

Initial version: 5 February 2007

1st revised version: 10 April 2007

2nd revised version: 19 April 2007

***Correspondence:**

Tsutomu Yamanaka

Terrestrial Environment Research Center, University of Tsukuba, Tsukuba 305-8577, Japan

Tel: +81-29-853-2538

Fax: +81-29-853-2530

E-mail: tyam@suiri.tsukuba.ac.jp

Abstract

We measured the stable isotopic composition of hydrogen (δD) within atmospheric water vapor collected simultaneously at six sites in the vicinity of a lake (Lake Kasumigaura, eastern Japan) to determine its spatial distribution characteristics and thereby diagnose sources and mixing of atmospheric moisture. The measured spatial distribution of δD showed no relation to distance from the lake, although it showed a correlation with the distribution of the water-vapor mixing ratio *Q*. For two of the three sampling days, we found a simple two-component (i.e., water vapor transpiring from local land surfaces and pre-existing vapor in the background atmosphere) mixing line in a Keeling plot (i.e., δ –1/*Q* diagram). On a third day, however, contributions from lake evaporation were detected in addition to the above components. On this day, lake-derived vapor accounted for approximately 10–20% of atmospheric water vapor at the sites located leeward of the lake. The observed differences in mixing patterns among sampling days can be explained by a simple atmospheric moisture budget. Thus, it is likely that simultaneous isotopic measurements of atmospheric water vapor at multiple locations with aid of Keeling plot are capable of giving us useful information in diagnosing the sources and mixing pattern of the vapor.

1. Introduction

Sources of precipitating water are important in revealing mechanisms that lead to variations in precipitation (Eltahir and Bras, 1996; Bosilovich, 2002; Sudradjat et al., 2003; James et al., 2004), especially in evaluating the impacts of lakes (Gat et al., 1994; Machavaram and Krishnamurthy, 1995; Burnett et al., 2004) and large-scale irrigation projects (Stidd, 1975; Barnston and Schickedanz, 1984) on local precipitation. Water isotopes (hydrogen and oxygen stable isotopes in water molecules) are useful tracers in identifying source areas of precipitating water (Yamanaka et al., 2002, 2004) and for evaluating the relative contributions of precipitating water from different sources (Gat et al., 1994). For these purposes, isotopes in precipitation are commonly used, but few studies have considered isotopes in atmospheric water vapor because of the complicated sampling procedure involved in such an approach. Notwithstanding these sampling problems, the isotopic composition of water vapor provides detailed and invaluable information on the sources of atmospheric moisture and subsequent mixing (Rozanski and Sonntag, 1982; Taylor, 1984; White and Gedzelman, 1984; Jacob and Sonntag, 1991; He et al., 2001; Gat et al., 2003; Lawrence et al., 2004). Such an approach will come into wider use in the near future with advances in rapid, in-situ measurement techniques using tunable laser (Webster and Heymsfield, 2003; Lee et al., 2005, 2006) or satellite remote-sensing techniques (Zakharov et al. 2004; Worden et al., 2007).

Fontes and Gonfiantini (1970) were among the first to evaluate the contribution of moisture evaporated from a lake to the atmosphere based on direct measurements of the isotopic composition of atmospheric water vapor. The authors partitioned atmospheric water vapor into a lake-origin component and a surrounding-land-origin component on the basis of their distinctive isotopic signatures. This simple two-component mixing analysis would be valid if there were only two sources; however, in many cases this assumption must be tested by

following a number of verification steps, as advected water vapor from outer regions may be present (Trenberth, 1999) and the isotopic signatures of evapotranspiring vapors from different land covers may be non-uniform.

The present paper describes a case study of the spatial distribution of deuterium in atmospheric water vapor in the vicinity of a lake, and presents an example of mixing analysis using the Keeling-plot method. The principal objectives of this study are to elucidate the regional-scale spatial variability of the isotopic signatures of water vapor and examine their usefulness in diagnosing the sources and mixing of atmospheric moisture.

2. Keeling-plot approach

The Keeling-plot approach was proposed by Keeling (1958, 1961) to identify the sources that contributed to increased concentrations of atmospheric CO_2 within forest canopies. Subsequently, many researches have used this method to analyze the one-dimensional vertical mixing of water vapors (e.g., Yakir and Wang, 1996; He and Smith, 1999) and to separately evaluate evaporation/transpiration components (e.g., Moreira et al., 1997; Yakir and Sternberg, 2000). The basis of this approach is the conservation of mass. Assuming that the atmospheric water vapor is an admixture of a background (i.e., non-local) component and an additional component produced by a local source, it is possible to obtain the following relationship by simultaneously solving conservation equations for water and water isotopes (Yakir and Wang, 1996):

$$\delta_v = a \times 1/Q_v + \delta_{ls}, \quad (1)$$

where $a = (\delta_{bg} - \delta_{ls})Q_{bg}$, Q (kg/kg) is the water vapor mixing ratio (or absolute humidity), δ (‰) is the isotopic composition expressed in the common δ-notation (i.e., $\delta = (R_{sample}/R_{standard} - 1)\times 10^3$, R is the D/H ratio, the standard is Vienna Standard Mean Ocean Water (VSMOW)),

and the subscripts *bg*, *ls*, and *v* denote the values for the background component, the local-source component, and atmospheric water vapor at an arbitrary height or horizontal location, respectively.

If δ_{bg}, δ_{ls}, and Q_{bg} are constant over the temporal and spatial scales of interest, then Eq. 1 represents a straight line in the δ_v versus $1/Q_v$ diagram (which is a version of the Keeling plot for water vapor), and its intercept corresponds to the isotopic composition of the local-source component. In other words, this approach assumes that temporal and spatial variations in δ_v reflect differences in the relative contribution of the local-source component contained within a unit mass of an air parcel. Although the assumptions that underlie the Keeling-plot approach are not always valid, it is possible to test their validity by considering the distribution of data plots; for instance, the linearity of the distribution confirms the invariance of δ_{bg}, δ_{ls}, and Q_{bg}.

In the case that two different local sources (*ls1* and *ls2*) contribute moisture to the atmosphere, the Keeling plot will show a straight line with an intermediate (exactly speaking, weighted mean) intercept between δ_{ls1} and δ_{ls2}; otherwise, data will plot within a triangle that is defined by three end-members with coordinates of ($1/ Q_{bg}$, δ_{bg}), (0, δ_{ls1}), and (0, δ_{ls2}), as presented by Moreira et al. (1997). Even if three or more local sources exist, the distribution of data within the plots provides a potential indication of the most effective source(s).

3. Study area and sampling strategy

The sampling of atmospheric water vapor for isotopic measurements was conducted in the summer of 2004 at six locations at varying distances from Lake Kasumigaura, eastern Japan (Fig. 1). Lake Kasumigaura is the second-largest lake in Japan, with a surface area of 219.9 km^2. The types of land use at each sampling site included grassland (Site A), rice paddy (Site C), vegetable fields (Site D), and parklands (Sites B, E, and F). Sites A, B, and C are situated

on uplands with elevations of approximately 25 m above mean sea level, while Sites C, E, and F are situated on alluvial lowlands with elevation ranging from 1 to 5 m.

Samples of water vapor were collected at a height above the ground of 1 m by pumping air at a flow rate of 3.5 L/min through a grass trap refrigerated at –196°C with liquid nitrogen. Water vapor was also sampled from the top of a 30 m tower at Site A, situated at the center of an experimental grassland run by the Terrestrial Environment Research Center (TERC) of the University of Tsukuba. This cryogenic trapping procedure for 1 to 1.5 hours allows us to collect water of 2 ml at least. The trap used had been demonstrated to be close to 100% efficient at water trapping and to introduce almost no error in deuterium measurement but non-negligible error in oxygen-18 measurement (Tsunakawa and Yamanaka, 2005). This is the reason why we did not adopt oxygen isotope measurement. (After the sampling experiments in the present study, the authors found that a very small amount of snow flakes, which has homogeneous deuterium content but remarkably heterogeneous oxygen-18 content, was escaping from the trap. They also confirmed that accuracy of oxygen isotope data could be improved if one used a trap holding metal beads.)

To determine the mixing ratio Q, air temperature and relative humidity were measured at each site at the same levels at which water vapor was sampled (i.e., 1 and 30 m), and recorded at 1-minute intervals using a micro-datalogger connected to a thermometer and hygrometer (HOBO RHTemp, Onset Computers Inc.) housed in a container that was ventilated and shielded from solar radiation. Preliminary experiments confirmed that the measurement error for Q was less than ±0.0004 kg/kg.

The stable isotopic composition of hydrogen within samples of water vapor was determined using an isotope ratio mass spectrometer (MAT252, Thermo Finnigan) at the University of Tsukuba, using the hydrogen gas equilibration method with a platinum catalyst. The total

error resulting from mass spectrometry analysis, sample preparation, and the cryogenic trapping of water vapor was less than ±1.0‰ (Tsunakawa and Yamanaka, 2005). In addition to samples of water vapor, we measured the isotopic compositions of a number of potential source waters: soil water within top 5-cm layer (Sites A, B, and D), surface water within the rice-paddy (Site C), and lake water (Sites E and F).

Table 1 provides a summary of the environmental conditions during each sampling period. Data at the lake shore (Fig. 1) were obtained at 4-m height above the lake surface by the National Institute for Environmental Studies (NIES, Japan) and published via the WWW (http://www-cger.nies.go.jp/kasumi/index.html). The lake evaporation rate was estimated using the bulk transfer equation with a transfer coefficient of 0.0012. For reference, Table 1 provides the evapotranspiration rate of the grassland, which is routinely measured by TERC using a weighing lysimeter and published via the WWW (http://www.suiri.tsukuba.ac.jp/hojyo/English/databaseE.html).

4. Results and discussion

The measured δD values for atmospheric water vapor and potential local source waters are summarized in Table 2. At Site A, measured δD of atmospheric water vapor (δ_v) at the top of a 30 m tower is lower than that at a height of 1 m, indicating that water vapor in the background atmosphere is relatively depleted in heavy isotopes. In other words, δ_v at ground level appears to reflect more strongly the isotopic signature of local-source vapor. Site-to-site variation in δ_v at a height of 1 m is greater than the error level of δD measurement, suggesting that the variation is significant, although the pattern of the variation is not simple. In contrast to the result of Fontes and Gonfiantini (1970), we found no dependence of δ_v on proximity to the lake (Fig. 2).

The pattern of spatial variation in δ_v, however, is very similar to that of the mixing ratio Q (Fig. 3). Previous studies have also reported a positive correlation between δ_v and Q (or its alternative, such as specific or absolute humidity) based on time series data (White and Gedzelman, 1984) or vertical distribution data (for the atmospheric surface layer, Yakir and Wang, 1996; for the planetary boundary layer and the lower free atmosphere, He and Smith, 1999; for the lower troposphere, Taylor, 1984). The present study may be the first to demonstrate a similarity between δ_v and Q variations based on spatial distribution data.

It is difficult to explain the origin of the spatial distribution of δ_v if we focus only on δ values, but Keeling plots provide some useful insights. Surprisingly, for two of the sampling days in July, the Keeling plot shows a clear liner relationship between δD and $1/Q$ (Fig. 4), and its regression line has a high determination coefficient (0.884 for 19 July and 0.912 for 26 July). This result indicates that the spatial variation in δ_v originated from a simple mixing of two components; that is, variations in δ_v among different sites reflect differences in the contribution ratio of the components. The intercepts of the regression lines and their standard error of estimate show that the δ value of the effective local-source vapor is –44.0±12.5‰ for 19 July and –35.8±10.3‰ for 26 July. These values largely correspond with the δD of soil waters and surface waters (see also Table 2b), indicating that the local-source vapor is principally produced by transpiration from land surfaces, which is not accompanied by isotopic fractionation (e.g., Ehleringer and Dawson, 1992).

Only for 14 June the Keeling plot provide two distinct regression lines (Fig. 5): one is for western sites and the other for eastern sites. The intercept of the former line is –44.4±3.6‰, very similar to δD for soil/surface waters (see also Table 2b) as in the other two days described above. In contrast, the intercept of the line for eastern sites close to the lake shows an intermediate δD value (–86.7±11.4‰) between that of soil/surface waters (–40 to –62‰)

and that of lake evaporation flux (–103.8‰), suggesting that the lake contributed a considerable amount of moisture to the atmosphere in the vicinity of the lake. Here, the isotopic composition of lake evaporation flux (δ_E) was estimated using the following Craig–Gordon model (Craig and Gordon, 1965):

$$\delta_E = \frac{\delta_w / \alpha_{eq} - h^* \delta_v - \varepsilon}{1 - h^* + 10^{-3} \Delta\varepsilon}, \quad (2)$$

where α_{eq} is the equilibrium fractionation factor, δ_w is the isotopic composition of lake water, h^* is the air relative humidity normalized by the saturation vapor pressure at the lake surface temperature, ε (= $(1–1/\alpha_{eq})\times10^3+\Delta\varepsilon$) is the total effective enrichment factor, $\Delta\varepsilon$ (= $C_k(1–h^*)$) is the kinetic enrichment factor, and C_k is a semi-empirical parameter (representative value of typical lake evaporation conditions is 12.5‰; Gonfiantini, 1986). In calculating Eq. 2, h^* was computed from NIES data (Table 1), and δ_v was given as observed value at Site F. Although there may be some uncertainties in determining δ_E (e.g., value of C_k and measurement location/height of parameters in Eq. 2), the difference between δ_E and δ values of atmospheric water vapor and soil/surface waters is remarkably clear.

We now seek to estimate the relative contribution of lake-origin vapor. Assuming that the isotopic signature of the effective local-source vapor (δ_{ls}) (determined as the intercept of the regression line for Sites D, E, and F) formed by the mixing of vapor evaporating from the lake (with isotopic composition δ_E) and that transpiring from land surfaces (with isotopic composition δ_T, determined as the intercept of the regression line for the western sites), the ratio of the lake-evaporation component (Q_E) to local-source vapors (Q_{ls}) can be calculated using a two-end-member mixing model (e.g., Phillips and Gregg, 2001):

$$\frac{Q_E}{Q_{ls}} = \frac{\delta_{ls} - \delta_T}{\delta_E - \delta_T}. \quad (3)$$

Given that δ_{ls} = –86.7±11.4‰, δ_T = –44.4±3.6‰, and δ_E = –103.8‰ as shown above, the

relative contribution of lake evaporation is estimated to be 71% of the local-source vapors. Standard error (SE) of this estimate is calculated to be 4% by an error propagation formula of Phillips and Gregg (2001). Similarly, the ratio of local-source vapor to total atmospheric water vapor (Q_{vs}) is given as:

$$\frac{Q_{ls}}{Q_v} = \frac{\delta_v - \delta_{bg}}{\delta_{ls} - \delta_{bg}}, \quad (4)$$

where δ_{bg} is the isotopic composition of the background component. If we assume that δ_{bg} is represented by the intersection point of the two regression lines in Fig. 5 (i.e., –126.7‰), then the relative contribution of the local-source component is estimated to be 22±6% as an average ± SE for Sites D, E, and F (i.e., δ_v = –117.7±0.9‰; see Table 2a). Consequently, we estimate that 16±4% of the atmospheric water vapor present at the sites is derived from lake evaporation. (Although an error analysis in the above did not consider uncertainties in δ_E and δ_{bg}, the SE of Q_E/Q_v is no more than 7% even if SEs of δ_E and δ_{bg} are ±10‰, respectively.)

We only detected a considerable contribution from lake evaporation on 14 June. It is important to consider why we were unable to detect such a contribution on the other two days (in July). Although temperature conditions differed between June and July, the water vapor fluxes were similar for the two months (Table 1). One important difference between the two sampling periods may be wind direction. On 14 June, when the wind direction was east-southeast, Sites D, E, and F were situated leeward of the lake, and the travel distance across the lake for an air parcel was more than 16 km. In contrast, the two sampling days in July recorded south-southwesterly winds. Under these conditions, Site E is no longer situated on the leeward side of the lake, and air parcels that reach Sites D and F travel a shorter distance (approximately 3 km) across the lake than air parcels on 19 June. Therefore, we consider that the contribution ratio of lake evaporation varies with wind direction.

Given an air column with a basal area of 1 m^2, a height of 100 m, density of 1.2 kg/m^3, and

a mixing ratio of 0.010 kg/kg (corresponding to the condition over the lake on 14 June), the initial content of water vapor within the column is computed to be 1.2 mm. If the column moves laterally at a speed of 6 m/s over a distance (L) of 16 km across the lake, for which the evaporation rate is 0.24 mm/hr, then the water vapor supplied by lake evaporation to the column is 0.18 mm, equivalent to 15% of the initial vapor content. Similar computations for the two days in July (but with L = 3 km) demonstrate that lake evaporation contributed very little water vapor to the air column on those days (2% on both 19 and 26 July). These results provide a quantitative explanation of the differences in the relative contribution of lake evaporation recorded for the sampling days in June and July. The results also suggest that high temperatures and humid conditions in July make it difficult to detect the isotopic signature of lake evaporation. It should be noted that because the assumed height of the air column in the calculated moisture budget is arbitrary, absolute values of computed lake-evaporation-contribution will vary depending on the chosen column height (in other words, vertical mixing strength). However, the agreement between the values derived from the isotopic approach (16±4%) and the simple atmospheric moisture budget (15%) may indicate that the vertical mixing of water vapors on 14 June had a scale of approximately 100 m.

Finally, it is worth reconsidering the isotopic signatures of the local-source and background components. According to Yamanaka et al. (2005), soil evaporation from grasslands is limited where the leaf area index (LAI) is greater than unity. While the evaporation flux from rice-paddies, which are usually covered by shallow water, is expected to be non-negligible, transpiration is probably still more dominant because the LAI is greater than unity during June and July (Hamada et al., 2004). Therefore, it is reasonable that in most cases, the isotopic signature of the effective local source corresponds to that of the transpiration flux.

That is, although the isotopic signature of the local source may vary spatially depending on land use or other surface/subsurface conditions, minor spatial variations would be destroyed by lateral airflow and vertical mixing. If land-surface conditions were almost uniform across a large enough area, it would be impossible to distinguish background atmospheric water vapor from local-source vapor. In the present study, however, the δ of the background component was lower than that of both transpiration flux and lake evaporation flux. In general, as water vapor that evaporates from the ocean is enriched in heavy isotopes relative to lake-origin vapor, low values of δ_{bg} would not reflect evaporation from the ocean. Thus, the δ value of the background component appears to reflect δ_v in the upper air, which is affected in turn by the in-cloud rainout process (Dansgaard, 1964; Rozanski and Sonntag, 1982; Taylor, 1984), or in the air mass exposed to precipitation along the trajectory upwind from the study area (Lawrence et al., 2004). It is interesting that δ_v at Site B was always close to δ_{bg}, although the reason for this is unknown. In addition, we may find that δ_{bg} varies spatially if we had focused on a larger spatial scale (e.g., >100 km). It is therefore necessary to further investigate processes that lead to the formation of δ_{bg}.

5. Summary and conclusions

The spatial distribution of δD for atmospheric water vapor is not simple and shows no dependence upon distance from the lake. Nevertheless, Keeling plot of the data indicates effective vapor-sources and their mixing pattern, suggesting that the spatial distribution of water-vapor δD is a reflection of spatial differences in the contribution ratios of the different components. The results of a water-vapor mixing analysis based on the Keeling plot are generally consistent with the results of a simple atmospheric moisture budget; accordingly, it is likely that multi-location measurements of isotopes in atmospheric water vapor are useful

in diagnosing the sources and mixing of atmospheric moisture. Although this study presents three observational results from which only one case showed detectable lake-origin vapor, further case studies under different conditions are needed to confirm the reliability and limitations of this approach. Improvements in the employed methodology will be helpful in addressing both the effects of lake/irrigation on local precipitation and the influence of various aspects of meso-scale atmospheric moisture circulation on variations in precipitation.

Acknowledgements

This research was supported by a Grant-in-Aid for Scientific Research (No. 15740289, TY). The authors express their gratitude to all the people who helped in taking samples of water vapor. This manuscript has greatly benefited from thoughtful comments of Juske Horita, Jim Lawrence, and an anonymous reviewer.

References

Barnston, A.G., Schickedanz, P.T., 1984. The effect of irrigation on warm season precipitation in the southern Great Plains. Journal of Climate and Applied Meteorology 23, 865-888.

Bosilovich, M.G., 2002. On the vertical distribution of local and remote sources of water for precipitation. Meteorology and Atmospheric Physics 80, 31-41.

Burnett, A.W., Mullins, H.T., Patterson, W.P., 2004. Relationship between atmospheric circulation and winter precipitation $\delta^{18}O$ in central New York State, Geophysical Research. Letters 31, 22209, doi:10.1029/2004GL021089.

Craig, H., Gordon, L.I., 1965. Deuterium and oxygen 18 variations in the ocean and the marine atmosphere. In: Tongiorgi E. (Ed.), Stable Isotopes in Oceanographic Studies and Paleotemperatures, Spoleto, Italy, pp. 9-130.

Dansgaad, W., 1964. Stable isotopes in precipitation. Tellus 16, 436-468.

Ehleringer, J.R., Dawson, T.E., 1992. Water uptake by plants: perspectives from stable isotope composition. Plant Cell Environment 15, 1073-1082.

Eltahir, E.A.B., Bras, R.L., 1996. Precipitation recycling. Reviews of Geophysics 34, 367-378.

Fontes, J.-Ch., Gonfiantini, R., 1970. Comparison isotopique et origine de la vapeur d'eau atmospherique dans la region du lac leman. Earth and Planetary Science Letters 7, 325-329.

Gat, J.R., Bowser, C.J., Kendall, C., 1994. The contribution of evaporation from the Great Lakes to the continental atmosphere: estimate based on stable isotope data, Geophysical Research Letters 21, 557-560.

Gat, J.R., Klein, B., Kushnir, Y., Roether, W., Wernli, H., Yam, R., Shemesh, A., 2003, Isotope composition of air moisture over the Mediterranean Sea: an index of the air-sea

interaction pattern. Tellus 55B, 953-965.

Gonfiantini, R., 1986. Environmental isotopes in lake studies. In: Fritz P., Fontes J.Ch. (Eds.), Handbook of Environmental Isotope Geochemistry, Vol. 2, Elsevier, New York, pp. 113-168.

Hamada, Y., Yabusaki, S., Tase, N., Taniyama, I., 2004. Stable isotope ratios of hydrogen and oxygen in paddy water affected by evaporation. Journal of Japanese Association of Hydrological Science 34, 209-216. (in Japanese)

He, H., Smith, R.B., 1999. Stable isotope composition of water vapor in the atmospheric boundary layer above the forests of New England. Journal of Geophysical Research 104, 11657-11673.

He, H., Lee, X., Smith R.B., 2001. Deuterium in water vapor evaporated from a coastal salt marsh. Journal of Geophysical Research 106, 12183-12191.

Jacob, H., Sonntag, C., 1991. An 8-year record of the seasonal variation of ^{2}H and ^{18}O in atmospheric water vapour and precipitation at Heidelberg, Germany. Tellus 43B, 291-300.

James, P., Stohl, A., Spichtinger, N., Eckhardt, S. and Forster, C., 2004. Climatological aspects of the extreme European rainfall of August 2002 and a trajectory method for estimating the associated evaporative source regions. Natural Hazards and Earth System Sciences 4, 733-746.

Keeling, C.D., 1958. The concentration and isotopic abundance of atmospheric carbon dioxide in rural areas. Geochimica et Cosmochimica Acta 13, 322-334.

Keeling, C.D., 1961. The concentration and isotopic abundance of carbon dioxide in rural and marine air. Geochimica et Cosmochimica Acta 24, 277-298.

Lawrence, J.R., Gedzelman, S.D., Dexheimer, D., Cho, H-K., Carrie, G.D., Gasparini, R., Anderson, C.R., Bowman, K.P., Biggerstaff, M.I., 2004. Stable isotopic composition of

water vapor in the tropics. Journal of Geophysical Research 109, D06115, doi:10.1029/2003JD004046.

Lee, X., Sargent, S., Smith, R., Tanner, B., 2005. In-situ measurement of water vapour $^{18}O/^{16}O$ isotope ratio for atmospheric and ecological applications. Journal of Atmospheric and Oceanic Technology 22, 555-565.

Lee, X., Smith, R., Williams, J., 2006. Water vapour $^{18}O/^{16}O$ isotope ratio in surface air in New England, USA. Tellus 58B, 293-304.

Machavaram, M.V., Krishnamurthy, R.V., 1995. Earth surface evaporative process: a case study from the Great Lakes region of the United States based on deuterium excess in precipitation. Geochimica et Cosmochimica Acta 59, 4279-4283.

Moreira, M.Z., Sternberg, L.daS.L., Martinelli, L.A., Victoria, R.L., Barbosa, E.M., Bonates, L.C.M., Napstad, D.C., 1997. Contribution of transpiration to forest ambient vapour based on isotopic measurements. Global Change Biology 3, 439-450.

Phillips, D.L., Gregg, J.W., 2001. Uncertainty in source partitioning using stable isotopes. Oecologia 127, 171-179.

Rozanski, K., Sonntag, C., 1982. Vertical distribution of deuterium in atmospheric water vapour. Tellus 34, 135-141.

Stidd, C.K., 1975. Irrigation increases rainfall ? Science 188, 279-280.

Sudradjat, A., Brubacker, K.L., Dirmeyer, P.A., 2003. Interannual variability of surface evaporative moisture sources of warm-season precipitation in the Mississippi River basin. Journal of Geophysical Research 108, 8612, doi:10.1029/2002JD003061.

Taylor, C.B., 1984. Vertical distribution of deuterium in atmospheric water vapour: problems in application to assess atmospheric condensation models. Tellus 36B, 67-72.

Trenberth, K.E., 1999. Atmospheric moisture recycling: role of advection and local

evaporation. Journal of Climate 12, 1368-1381.

Tsunakawa, A., Yamanaka, T., 2005. Reliability of water vapor collection method for stable isotope determination, Journal of Japan Society of Hydrology & Water Resources 18, 306-309. (in Japanese)

Worden, J., Noone, D., Bowman, K., the Tropospheric Emission Spectrometer science team and data contributors, 2007. Importance of rain evaporation and continental convection in the tropical water cycle. Nature 445, 528-532.

Webster, C.R., Heymsfield, A.J., 2003. Water isotope ratios D/H, $^{18}O/^{16}O$, $^{17}O/^{16}O$ in and out of clouds map dehydration pathways. Science 302, 1742-1745.

White, J.W.C., Gedzelman, S.D., 1984. The isotopic composition of atmospheric water vapor and the concurrent meteorological conditions. Journal of Geophysical Research 89, 4937-4939.

Yakir, D., Sternberg, L.daS.L., 2000. The use of stable isotopes to study ecosystem gas exchange. Oecologia 123, 297-311.

Yakir, D., Wang, X.-F., 1996. Fluxes of CO_2 and water between terrestrial vegetation and the atmosphere estimated from isotope measurements. Nature 380, 515-517.

Yamanaka, T., Shimada, J., Miyaoka, K., 2002. Footprint analysis using event-based isotope data for identifying source area of precipitated water. Journal of Geophysical Research 107(D22), 4624, doi:10.1029/2001JD001187.

Yamanaka, T., Shimada, J., Hamada, Y., Tanaka, T., Yang, Y., Wanjun Z., Chunsheng, H., 2004. Hydrogen and oxygen isotopes in precipitation in a northern part of the North China Plain: climatology and inter-storm variability. Hydrological Processes 18, 2211－2222.

Yamanaka, T., Tsunakawa, A. Smith, R.B., 2005. Isotopic measurement of evapotranspiration flux and its use for partitioning evaporation/transpiration components. Proceedings of 2005

Annual Conference, Japan Society of Hydrology and Water Resources, 78-79. (in Japanese)

Zakharov, V.I., Imasu, R., Gribanov, K.G., Hoffmann, G., Jouzel, J., 2004. Latitudinal distribution of the deuterium to hydrogen ratio in the atmospheric water vapor retrieved from IMG/ADEOS data. Geophysical Research Letters 31, 12104, doi:10.1029/2004GL019433.

Table 1 Environmental conditions during the three sampling periods

Date 2004	Time JST	T_a* (°C)	RH* (%)	T_w* (°C)	U* (m/s)	WD*	E_{lake} (mm/hr)	ET_{grass} (mm/hr)
14 June	15:00–16:30	23.3	58	23.4	6.0	ESE	0.24	0.42
19 July	12:00–13:30	31.2	58	29.2	4.7	SSW	0.22	0.35
26 July	11:00–12:00	31.2	58	29.5	4.2	SSW	0.20	0.45

JST: Japanese standard time, T_a: air temperature, RH: relative humidity, T_w: surface water temperature, U: wind speed, WD: wind direction, E_{lake}: evaporation rate from Lake Kasumigaura estimated by the bulk transfer equation, ET_{grass}: evapotranspiration rate from grassland measured by a weighing lysimeter at Site A (Terrestrial Environment Research Center, University of Tsukuba).

* Data observed at the lake shore point (see Fig. 1) by the National Institute for Environmental Studies (NIES).

Table 2 Deuterium contents (δD) of atmospheric water vapor and soil/surface waters at six sampling sites for each sampling day. Water vapor mixing ratio (*Q*) is also given.

(a) Atmospheric water vapor

Site	Sampling height (m)	δD (‰)			*Q* (g/kg)		
		14 June	19 July	26 July	14 June	19 July	26 July
A	1	–114.8	–104.6	–103.5	10.3	18.6	17.0
A’	30	–124.2	–121.1	–114.6	9.0	15.1	14.7
B	1	–127.1	–119.6	–116.2	8.7	14.5	14.3
C	1	–113.0	–111.5	–109.1	10.4	16.0	15.7
D	1	–119.9	–113.1	–107.3	10.6	15.4	15.3
E	1	–117.0	N/A	–115.3	11.2	N/A	14.6
F	1	–116.3	–105.4	–105.2	11.9	17.7	16.7

(b) Soil/surface waters

Site	Type	δD (‰)		
		14 June	19 July	26 July
A	Soil water*	–61.5	–42.7	N/A
B	Soill water*	–54.8	N/A	N/A
C	Surface water	–39.7	–29.7	–35.0
D	Soil water*	–48.9	-40.5	–34.4
E	Lake water	–36.9	N/A	–32.6
F	Lake water	–32.6	–31.5	–28.1

* Values for top 5-cm soil layer.

Figure captions

Figure 1. Study area and location of sampling sites. Star indicates the lake shore observation point of NIES (36°00’13.2”N, 140°22’51.0”E). The coordinates of Site A are 36°06’48.6”N and 140°05’51.8”E.

Figure 2. Spatial distribution of deuterium content (δD) in atmospheric water vapor sampled at a height of 1 m.

Figure 3. Spatial distribution of water-vapor mixing ratio (*Q*) at a height of 1 m.

Figure 4. Keeling plot describing the relationship between water vapor δD and the inverse of the mixing ratio on 19 July (upper) and 26 July (lower). Data labels indicate sampling sites. Horizontal bars represent the measurement error involved in determining the mixing ratio. Dashed lines represent the best fit for all data by found by linear regression. Vertical bars attached to solid diamond denote standard error of *y*-intercept of the regression line. δD values for possible source waters are also shown.

Figure 5. As for Figure 4 but for 14 June. Two regression lines are described: one for western sites (black symbol) and another for eastern sites close to the lake (gray symbol).

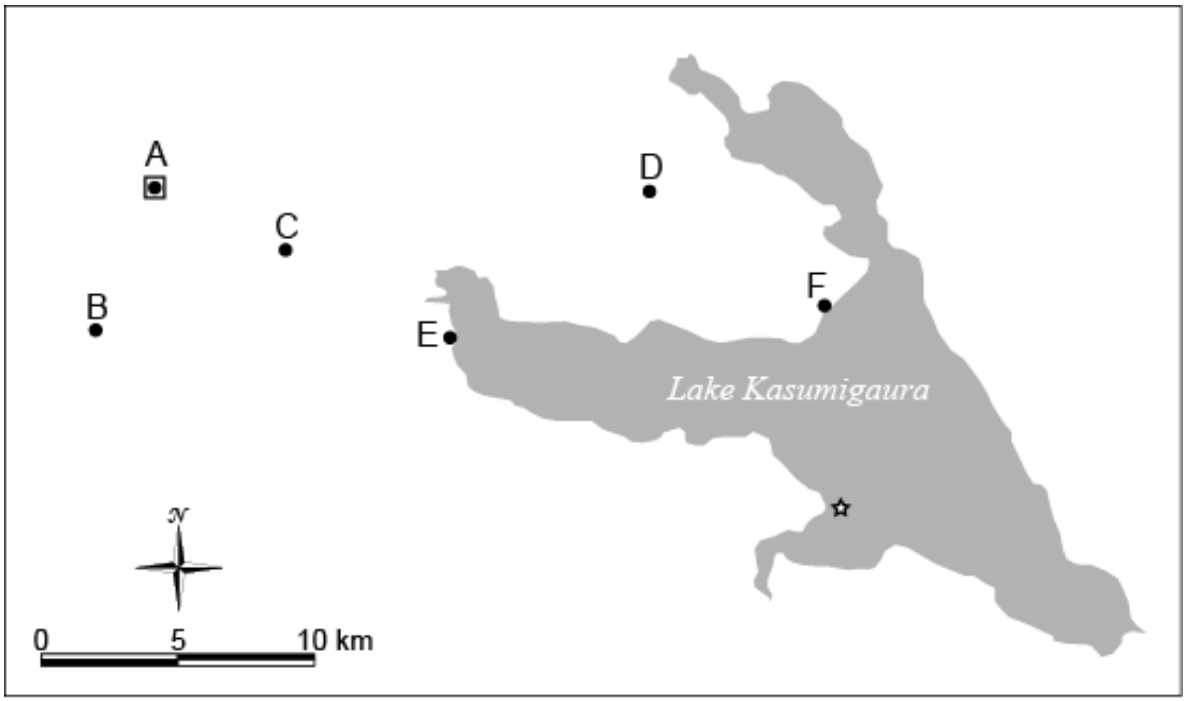

Figure 1. Map of study area and location of sampling sites. Star indicates the lake observation point of NIES (36°00’13.2”N, 140°22’51.0”E). The coordinates of Site A are 36°06’48.6”N and 140°05’51.8”E.

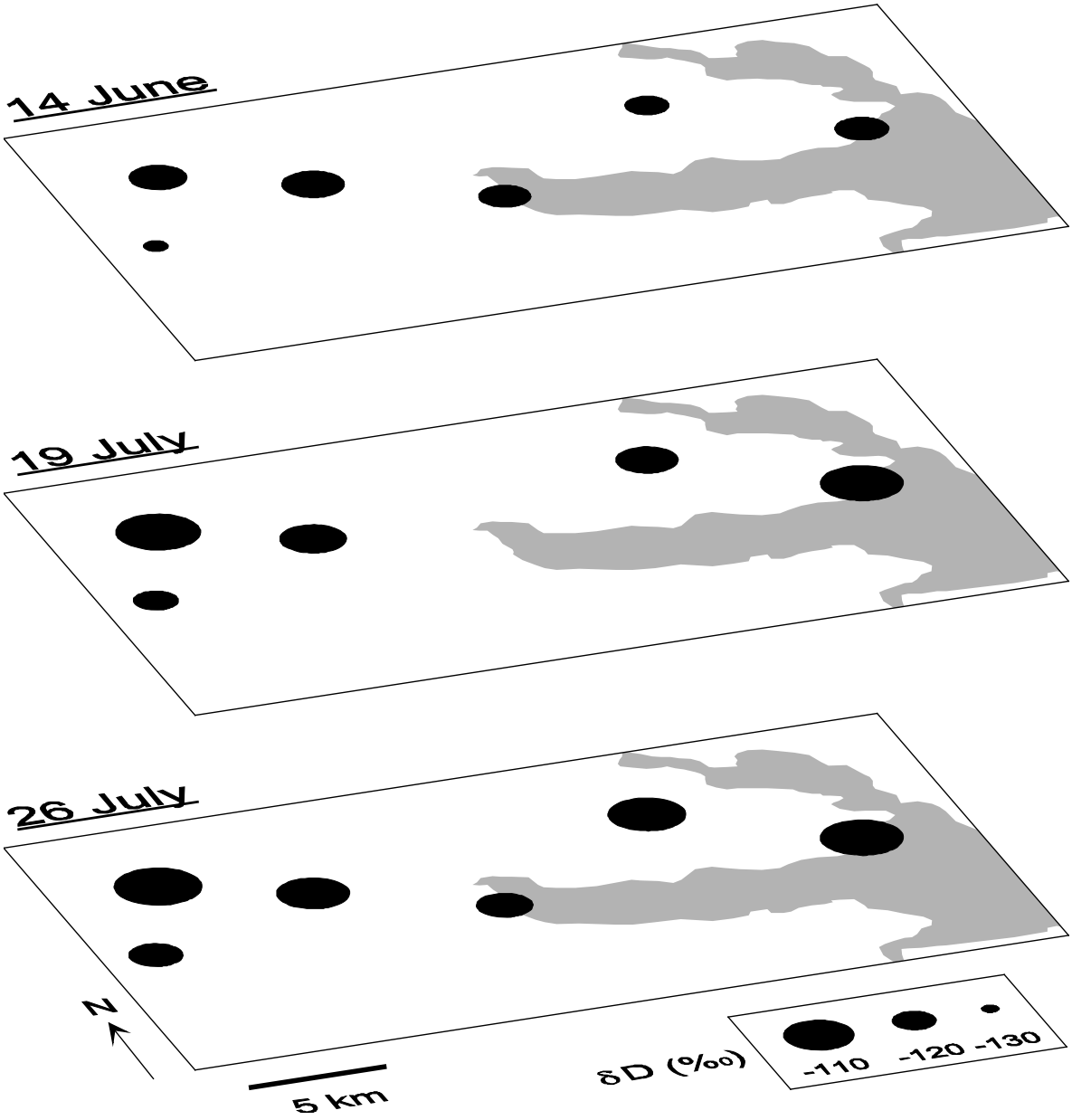

Figure 2. Spatial distribution of deuterium content (δD) in atmospheric water vapor sampled at a height of 1 m.

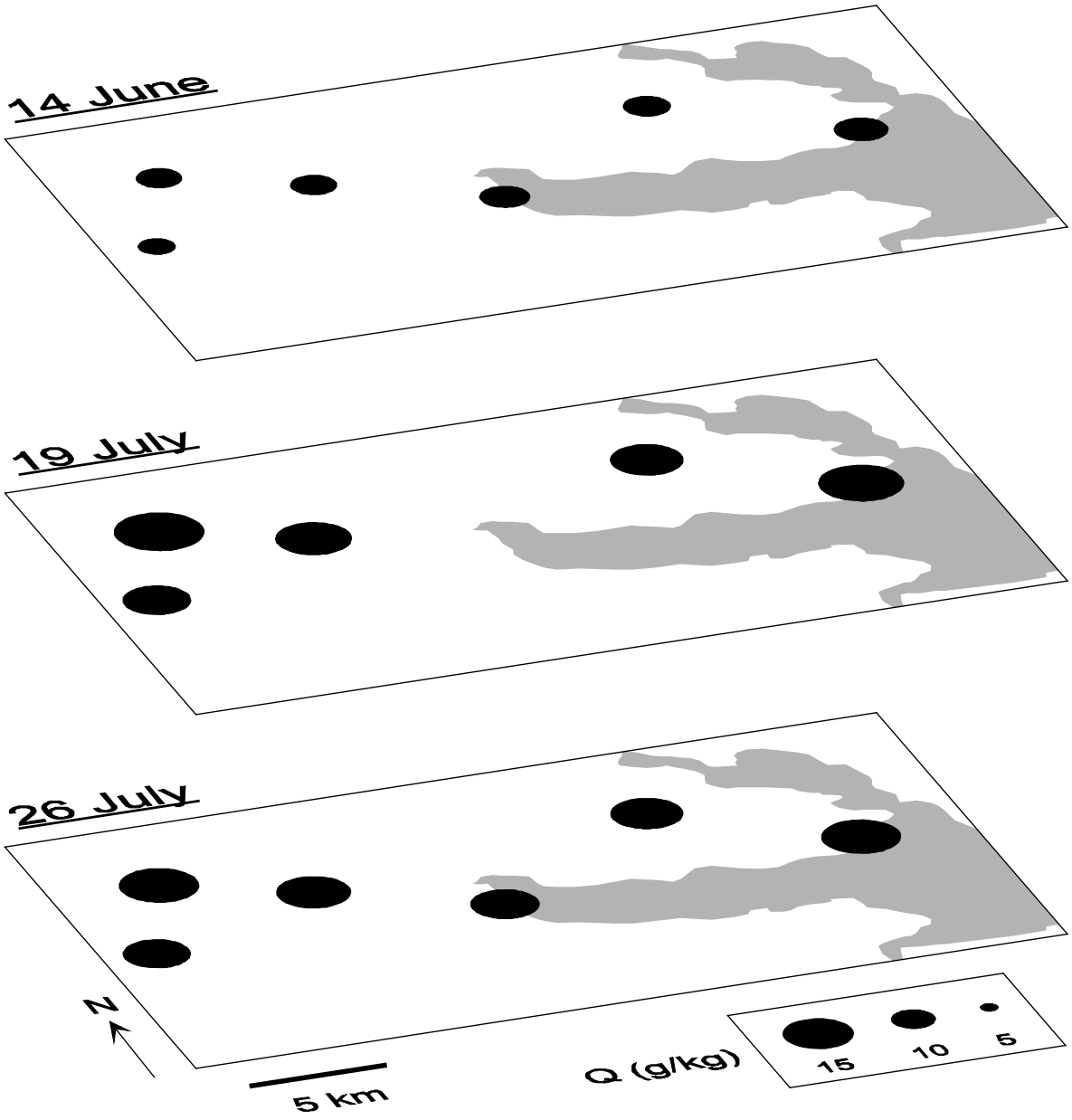

Figure 3. Spatial distribution of water-vapor mixing ratio (Q) at a height of 1 m.

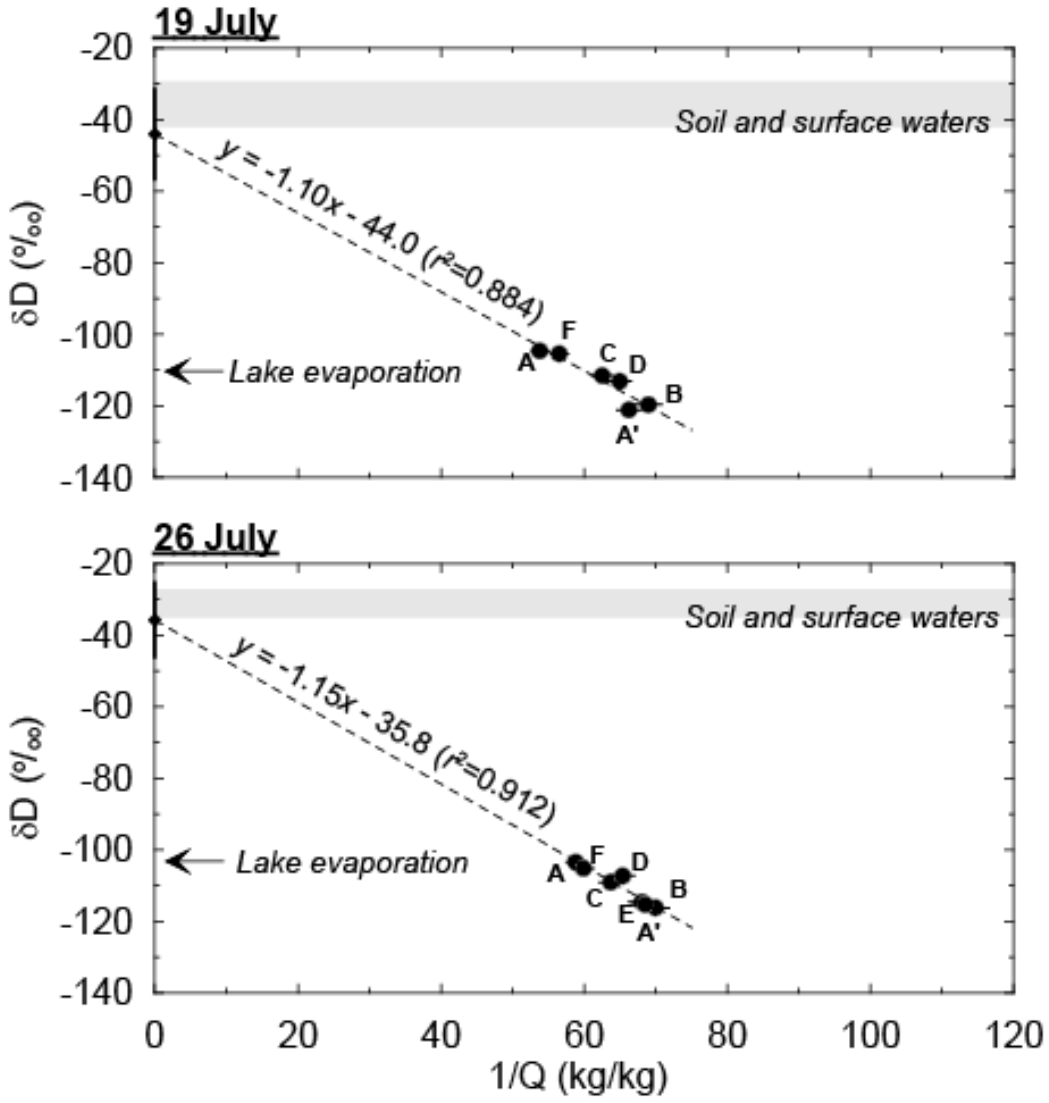

Figure 4. Keeling plot describing the relationship between water vapor δD and the inverse of the mixing ratio on 19 July (upper) and 26 July (lower). Data labels indicate sampling sites. Horizontal bars represent the measurement error involved in determining the mixing ratio. Dashed lines represent the best fit for all data by found by linear regression. Vertical bars attached to solid diamond denote standard error of *y*-intercept of the regression line. δD values for possible source waters are also shown.

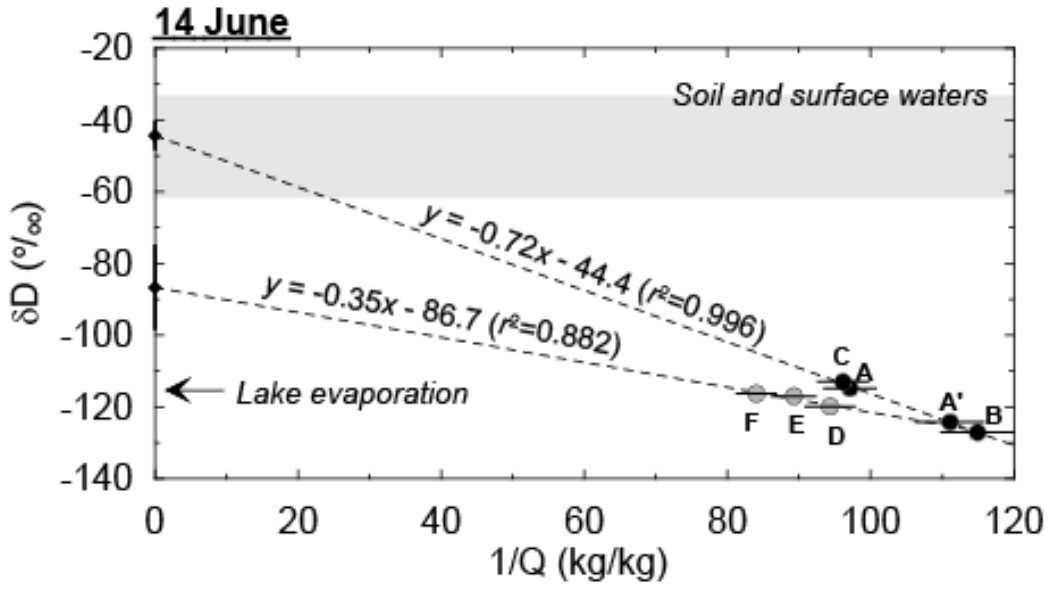

Figure 5. As for Figure 4 but for 14 June. Two regression lines are described: one for western sites (black symbol) and another for eastern sites close to the lake (gray symbol).